

Evidence concerning the origins of the observed diastereoselectivity was obtained by repeating the reaction using 50% MeOH-*d*<sub>4</sub>/THF as solvent. In this case, anodic oxidation of **1** led to a 68% yield of cyclized products. Compounds **2** and **3** were again formed in a 5.3:1 ratio (the compounds had OCD<sub>3</sub> acetals). NMR analysis showed that approximately 50% of the cyclized material still had an OCH<sub>3</sub> group at the benzylic position and therefore had to be derived from intramolecular transfer of the methoxy group originally at C<sub>1</sub> of the starting material. This material was predominately (greater than 10:1) the *cis* and *trans* major products, **2**. The remainder of the material had an OCD<sub>3</sub> group at the benzylic position and was formed in a ca. 2:1 ratio of cyclized products **2** and **3**. These products are assumed to arise from solvent trapping of an incipient benzylic carbocation.

The methanol-*d*<sub>4</sub> experiment suggests that the bulk of the diastereoselectivity was derived from an intramolecular transfer of the C<sub>1</sub> methoxy group and that at one point half of the material must pass through a bicyclic intermediate like **6** (Scheme I). The stereochemistry of the major products can be explained by suggesting that the phenyl ring occupies the sterically least hindered position in this bicyclic intermediate. Although the possibility of a *trans*-fused bicyclic intermediate is troublesome, OCH<sub>3</sub> ether products having both *cis* and *trans* stereochemistry about the five-membered ring are formed (1:1 ratio), and the lack of any deuterium incorporation at the bridgehead positions rules out the possibility of the *trans* product resulting from epimerization of a *cis* product. A mechanism wherein either **4** or **5** is trapped by solvent to form a mixed OCH<sub>3</sub>/OCD<sub>3</sub> acetal prior to migration seems unlikely in view of the difference in diastereomer ratios obtained for the OCH<sub>3</sub> and OCD<sub>3</sub> benzyl ether products.<sup>10</sup>

Having determined that the anodic oxidation of **1** could cleanly lead to intramolecular coupling products, we turned our attention to examining whether the enol ether, the styrene, or both groups were necessary for effective cyclization.<sup>11</sup> In order to address this question, we synthesized cyclization substrates **7a** and **7b**. Preparative electrolysis of **7a** in methanol led to the formation of a 77% isolated yield of cyclized products (Scheme II). These products were obtained in a ca. 3.5:1 ratio of compounds **8a** and **9a**. No uncyclized material was obtained. On the other hand, anodic oxidation of **7b** in methanol led to a complex mixture of products. From the 300-MHz <sup>1</sup>H NMR spectrum of the crude reaction mixture it was clear that the majority of the material was not cyclized. From the mixture, four major compounds were obtained along with 6% of the recovered starting material. Two of the compounds were uncyclized and were isolated in 25% yield. A 20% yield of cyclized materials was obtained. It is clear from these results that anodic oxidation of the enol ether is much more effective at initiating the intramolecular coupling reactions than is oxidation of the styrene moiety.

Finally, the reactions were studied in order to see if silyl enol ethers would be compatible with the electrochemical oxidation conditions. To this end, silyl enol ether substrates **7c** and **7d** were studied. Electrolysis of **7c** led to the formation of a 67% isolated yield of dimethoxy acetal products **8a** and **9a**. These products were obtained in a 2.6:1 ratio, respectively. Anodic oxidation of **7d** led to the formation of a 67% isolated yield of cyclized products **2**, **3**, and **8d**, along with 9% of the recovered starting material.

The products were obtained in a combined 1.8:1 mixture of isomers at the benzylic position. In neither case was any uncyclized material isolated. The use of silyl enol ether initiators should greatly expand the synthetic utility of the reactions because of the ease of their synthesis.

In summary, we have found that the intramolecular anodic coupling of enol ethers and olefinic nucleophiles can lead to high yields of cyclized products.<sup>12</sup> *These examples represent a new class of potentially useful anodic carbon-carbon bond forming reactions.* Studies aimed at further elucidating the factors that govern product formation and diastereoselectivity as well as determining the overall synthetic utility of these reactions are currently underway. The results of these studies will be reported in due course.

**Acknowledgment.** This work was supported by the donors of the Petroleum Research Fund, administered by the American Chemical Society, and by the Biomedical Research Support Program, Division of Research Resources, National Institutes of Health. We also gratefully acknowledge the Washington University High Resolution NMR Facility, partially supported by NIH 1S10R02004, the Washington University Mass Spectrometry Resource Center, partially supported by NIHRR00954, and Washington University's X-Ray Crystallography Facility, funded by the National Science Foundation's Chemical Instrumentation Program (Grant CHE-8811456), for their assistance.

**Supplementary Material Available:** A sample experimental procedure for the electrochemical cyclization reaction along with characterization data for compounds **1-3** and **7-10** and a structure determination summary for the 2,4-DNP derivative derived from **2** (18 pages); a list of observed and calculated structure factors for the 2,4-DNP derivative derived from **2** (25 pages). Ordering information is given on any current masthead page.

(12) Recently, a chemical variant to these reactions has been reported for phenyl-substituted silyl enol ethers. Snider, B. B.; Kwon, T. *Abstracts of Papers, 199th National Meeting of the American Chemical Society, Boston, MA; American Chemical Society: Washington, DC 1990; ORGN 322.*

## Models of the Cytochromes *b*. 7. Novel Features in the Proton Nuclear Magnetic Resonance Spectra of Mono-Ortho-Substituted Dialkylamido Tetraphenylporphyrinatoiron(III) Complexes

Hong Zhang, Ursula Simonis, and F. Ann Walker\*

Department of Chemistry and Biochemistry  
San Francisco State University  
San Francisco, California 94132

Received January 22, 1990

For some time it has been proposed that the effects of hindered axial ligand rotation and fixed axial ligand orientation may be significant for the regulation of midpoint potentials<sup>1</sup> and for the explanation of unusual shifts of certain resonances in the proton NMR spectra of heme proteins.<sup>2-4</sup> These suggestions have stimulated a number of investigations to determine the role of these effects in heme proteins and model heme compounds.<sup>5-10</sup>

(1) Korszun, Z. R.; Moffat, K.; Frank, K.; Cusanovich, M. A. *Biochemistry* **1982**, *21*, 2253-2258.

(2) (a) LaMar, G. N. *Biological Applications of Magnetic Resonance*; Shulman, R. G., Ed.; Academic Press: New York, 1979; pp 305-343. (b) McLachlan, S. J.; LaMar, G. N.; Lee, K. B. *Biochim. Biophys. Acta* **1988**, *957*, 430-445.

(3) LaMar, G. N.; Walker, F. A. *The Porphyrins*; Dolphin, D., Ed.; Academic Press: New York, 1979; Vol. IV, pp 61-157.

(4) Walker, F. A.; Benson, M. J. *Phys. Chem.* **1982**, *88*, 3495-3499.

(5) (a) Walker, F. A.; Emrick, D.; Rivera, J. E.; Hanquet, B. J.; Buttlare, D. H. *J. Am. Chem. Soc.* **1988**, *110*, 6234-6240. (b) Walker, F. A.; Huynh, B. H.; Scheidt, W. R.; Osvath, S. R. *J. Am. Chem. Soc.* **1986**, *108*, 5288-5297. (c) Walker, F. A.; Buehler, J.; West, J. T.; Hinds, J. L. *J. Am. Chem. Soc.* **1983**, *105*, 6923-6929.

(9) Crystallographic data for C<sub>20</sub>H<sub>22</sub>N<sub>4</sub>O<sub>5</sub>: mol wt 398.4; triclinic, space group P1̄ (No. 2); *a* = 7.236 (2) Å, *b* = 17.036 (6) Å, *c* = 17.134 (6) Å,  $\alpha$  = 86.03 (3)°,  $\beta$  = 82.64 (3)°,  $\gamma$  = 68.79 (2)°, *V* = 1953 (1) Å<sup>3</sup>,  $\rho$  = 1.355 g/cm<sup>3</sup> for *Z* = 4 at 22 °C,  $\mu$  = 0.93 cm<sup>-1</sup> (Mo K $\alpha$ ,  $\lambda$  = 0.71073 Å). A total of 7464 reflections were collected using SIEMENS R3m/V automated diffractometer. The structure was solved by direct methods. Full-matrix least-squares refinement using 3610 observed [*F* > 6*J*(*F*)] reflections out of 6868 unique reflections gave a final *R* = 0.0467 and *R*<sub>w</sub> = 0.0315.

(10) At this point no evidence has been obtained to indicate when the second electron is removed. The trapping of electrochemically generated radical cations with methoxy radicals is well preceded: Dolson, M. G.; Swenton, J. S. *J. Am. Chem. Soc.* **1981**, *103*, 2361. Nilsson, A.; Palmquist, U.; Pettersson, T.; Ronlan, A. *J. Chem. Soc., Perkin Trans. 1* **1978**, *7*, 708.

(11) Interestingly, both groups have similar oxidation potentials. For example, cyclic voltammetry of both **4a** and **4b** gives rise to an initial oxidation wave at +1.4 V vs a Ag/AgCl reference electrode (Pt anode/1 N LiClO<sub>4</sub> in CH<sub>2</sub>CN).

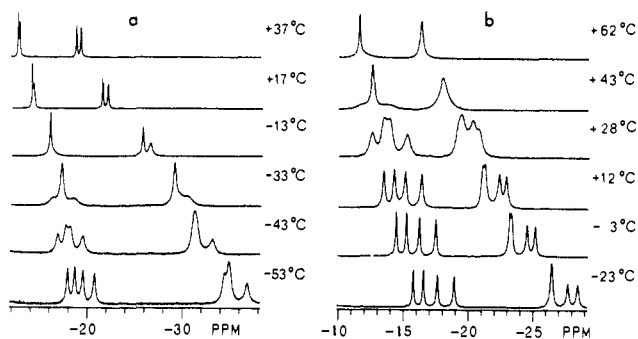
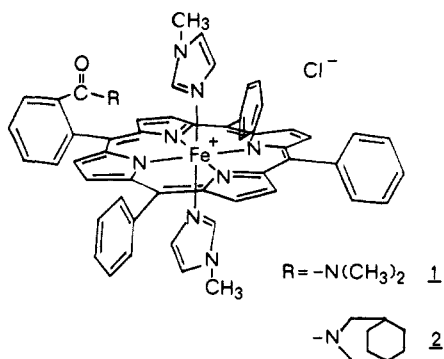


**Figure 1.** NMR spectra (300 MHz) (General Electric GN-300) of the pyrrole proton resonances of (a) complex 1 and (b) complex 2 as a function of temperature, both in  $\text{CDCl}_3$ . In 1 the coalescence from eight to two peaks occurs at around  $-27^\circ\text{C}$ , in 2 at approximately  $60^\circ\text{C}$ .

Our interest in evaluating the importance of hindered axial ligand rotation and fixed axial ligand orientation on the  $^1\text{H}$  NMR spectra of model heme compounds has led to the synthesis of two bis(*N*-methylimidazole)-iron(III) complexes (structures 1 and 2). The dialkylamide substituent is derived from either di-



methylamine or 3-azabicyclo[3.2.2]nonane. The synthesis and characterization of the free base porphyrins and their corresponding high-spin chloroiron(III) complexes will be described elsewhere.<sup>11</sup> In this report we present some novel features in the  $^1\text{H}$  NMR spectra of the low-spin iron(III) complexes which are related to hindered axial ligand rotation. The approach of unsymmetrical substitution with a bulky dialkylamide substituent accomplished our goal of hindering one axial ligand from free rotation and keeping it in a certain orientation at low temperatures. This, in combination with unsymmetrical substitution, has a profound effect on the pyrrole proton NMR resonances of the Fe(III) complexes. Depending on the bulk of the dialkylamide group, up to eight separate lines of equal intensities, divided into two groups of four signals each, separated by at least 6 ppm, are observed for the eight pyrrole protons. Variable-temperature measurements performed in  $\text{CDCl}_3$  and  $\text{CD}_2\text{Cl}_2$  solutions at 300 MHz, depicted in Figure 1, showed that each complex undergoes a kinetic exchange process. At low temperatures the spectral region of the pyrrole resonances of complexes 1 and 2 is split into a maximum of seven or eight signals, respectively. On heating,

these lines begin to coalesce to give (fortuitously) two or three broad resonances at intermediate temperatures (Figure 1), followed, for complex 1, by the eventual appearance of four sharp resonances at higher temperatures. For complex 2 the fast-exchange limit of four sharp signals cannot be achieved in the solvents used. Preliminary results of saturation transfer, two-dimensional exchange (EXSY), and rotating-frame cross-relaxation (ROESY) experiments all confirm that the pairs of peaks 1,4; 2,3; 5,8; and 6,7 are in chemical exchange, which accounts for the collapse of the eight-peak pattern to two or three broad signals in the intermediate-exchange region. Two-dimensional nuclear Overhauser studies (NOESY) at lower temperatures show not only chemical-exchange cross peaks but also through-space couplings within each group of four resonances.<sup>12</sup>

We believe that the novel eight-peak pattern and the unusually large spread of the signals for the pyrrole protons of 2 can only be explained by (a) the electronic effect of the substituent and (b) a specific orientation of the planar axial ligand at lower temperatures. The eight-peak pattern is not caused by the asymmetry of the *N*-methylimidazole ligand, since preliminary experiments utilizing 4-(dimethylamino)pyridine as a symmetrical axial ligand also reveal eight pyrrole resonances at lower temperatures. The occurrence of four peaks for complex 1 at the higher temperature limit results from free rotation of the axial ligand in proximity of the substituent, leaving only unsymmetrical substitution to create different electronic environments for the pyrrole protons. Earlier investigations<sup>13</sup> demonstrated that the electronic effect of one phenyl substituent splits the pyrrole resonance into at most four signals. At higher temperatures the larger substituent of complex 2 cannot undergo enough thermal motion to keep from partially hindering the rotation of the axial ligand which is close to the substituent.<sup>14</sup>

It has previously been suggested<sup>4</sup> that a planar axial ligand creates in-plane magnetic anisotropy due to the second-order Zeeman contribution to the dipolar shift.<sup>15,16</sup> Hence the effect of this hindered rotation, superimposed upon the effect of unsymmetrical substitution, explains the existence of eight pyrrole H resonances at lower temperatures, so long as the axial ligand plane is not fixed along the symmetry plane of the unsymmetrical porphyrin (or at  $90^\circ$  to it). We believe that the coalescence behavior of both complexes is caused by the increased mobility of the axial ligand as the temperature is raised, probably made possible by increased thermal motion of the substituent.<sup>14</sup> Curie plots of the seven or eight pyrrole resonances observed at low temperatures show changes in slope at about  $-40^\circ\text{C}$  for both complexes 1 and 2. The coordinated *N*-methylimidazole  $\text{CH}_3$  signals also change slopes slightly at about the same temperature for both compounds, suggesting a change in the degree of lifting of the degeneracy of  $d_{xz}$  and  $d_{yz}$  at that point. On the basis of these observations we are currently developing a theoretical model that will predict the relationship between the angular orientation of the hindered axial ligand at low temperatures and the pattern of pyrrole proton resonances observed, as well as the coalescence behavior.

From our studies to date we can conclude that the unique pyrrole resonance splitting pattern and the large spread of the signals, which to our knowledge have not previously been reported, offer new insights into the importance of restricted axial ligand rotation in model heme complexes. In addition, these results support the hypothesis<sup>2,4</sup> that axial ligand orientation cannot be overlooked in the interpretation of unusual NMR shift patterns in heme proteins.

(6) (a) Scheidt, W. R.; Osvath, S. R.; Lee, Y. L. *J. Am. Chem. Soc.* **1987**, *109*, 1958–1963. (b) Scheidt, W. R.; Kirner, J. F.; Hoard, J. L.; Reed, C. A. *J. Am. Chem. Soc.* **1987**, *109*, 1963–1968. (c) Scheidt, W. R.; Lee, Y. L. *J. Struct. Bonding (Berlin)* **1987**, *64*, 2–70. (d) Scheidt, W. R.; Chipman, D. M. *J. Am. Chem. Soc.* **1986**, *108*, 1163–1167. (e) Geiger, D. K.; Chunplang, V.; Scheidt, W. R. *Inorg. Chem.* **1985**, *24*, 4736–4741.

(7) (a) Soltis, S. M.; Strouse, C. E. *J. Am. Chem. Soc.* **1988**, *110*, 2824–2829. (b) Quinn, R.; Valentine, J. S.; Byrn, M. P.; Strouse, C. E. *J. Am. Chem. Soc.* **1987**, *109*, 3301–3308. (c) Quinn, R.; Strouse, C. E.; Valentine, J. S. *Inorg. Chem.* **1983**, *22*, 3934–3940.

(8) Traylor, T. G.; Berzinis, A. P. *J. Am. Chem. Soc.* **1980**, *102*, 2844–2846.

(9) Goff, H. *J. Am. Chem. Soc.* **1980**, *102*, 3252–3254.

(10) Nakamura, M.; Groves, J. T. *Tetrahedron* **1988**, *44*, 3225–3230.

(11) Simonis, U.; Zhang, H.; Kipp, C.; Walker, F. A., to be submitted.

(12) Simonis, U.; Walker, F. A., to be submitted.

(13) (a) Walker, F. A.; Balke, V. L.; McDermott, G. A. *J. Am. Chem. Soc.* **1982**, *104*, 1569–1574. (b) Walker, F. A.; Balke, V. L.; McDermott, G. A. *Inorg. Chem.* **1982**, *21*, 3342–3348. (c) Walker, F. A. *J. Am. Chem. Soc.* **1980**, *102*, 3254–3256.

(14) Axial ligand exchange does not affect the pyrrole H pattern of either compound up to the high-temperature limit of either solvent used. Hence, axial ligand exchange is not the cause of the coalescence of the eight peaks.

(15) Horrocks, W. D.; Greenberg, E. S. *Biochim. Biophys. Acta* **1973**, *322*, 38–44.

(16) Horrocks, W. D.; Greenberg, E. S. *Mol. Phys.* **1974**, *27*, 993–999.

**Acknowledgment.** This work was part of the M.S. Thesis Research of H. Z. (1988), San Francisco State University. It was supported by NIH Grant DK-31038 (F.A.W.) and by the NIH (RR 02684) and the NSF (DMB-8516065) for purchase of the NMR spectrometer.

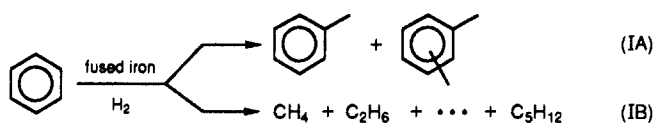
## Fused Iron Catalyzed Conversion of Benzene to Toluene

S. Mark Davis\* and Carl W. Hudson

Exxon Research and Development Laboratory  
P.O. Box 2226, Baton Rouge, Louisiana 70821

Received April 12, 1990

Whereas benzene hydrogenation catalyzed over group VIII metals has been investigated, intensively,<sup>1,2</sup> very few reports<sup>3</sup> have considered ring hydrogenolysis of this simple aromatic hydrocarbon. We have recently discovered that *surface carbon reincorporation* to produce toluene and xylenes (reaction IA) is an important reaction operating during benzene hydrogenolysis (reaction IB) over a conventional fused iron ammonia synthesis catalyst. Intrinsic selectivity for the novel reaction IA is sub-



stantial over a wide range of temperatures; however, synthetic utility is limited by secondary reactions involving preferential conversion of alkylbenzenes. Benzene conversion is accompanied by carbiding of the catalyst near surface region.

Reaction studies were carried out at atmospheric pressure in an apparatus equipped with a microflow reactor and a surface analysis system with capabilities for X-ray photoemission (XPS) and low energy helium ion scattering (LEIS).<sup>4</sup> Research grade H<sub>2</sub> was used as supplied, whereas benzene (MCB, "thiophene-free") was filtered over activated alumina, freeze-pumped, and purged with dry H<sub>2</sub> before use. The BASF-R catalyst exhibited a nominal composition (wt %) of 2-3% Al<sub>2</sub>O<sub>3</sub>, 0.6-1.0% K<sub>2</sub>O, 1.0-1.5% CaO, and 95% free iron. Catalysts were activated by H<sub>2</sub> treatment at 490-500 °C for 1 h, an XPS spectrum was recorded, and the catalyst was returned to the reactor. After 0.5-15 h of reaction time, the catalyst was cooled to 70 °C before evacuation of the gas mixture and recording of another XPS spectrum. Subsequently, the reactivity of carbon deposits was explored by using temperature-programmed hydrogen treatment (TPHT) wherein the catalyst was heated in flowing H<sub>2</sub> at a rate of 5 K/min, and the evolution of hydrocarbons was detected with a gas chromatograph.

Initial rates and product distributions for benzene conversion at 280-380 °C and at several conversion levels are compared in Table I. Toluene and methane were major products along with small yields of C<sub>2</sub>-C<sub>5</sub> alkanes and xylenes in an approximate 1:2:2

**Table I.** Rates and Product Distributions for Benzene Conversion over BASF Fused Iron<sup>a</sup>

reactn T, °C	reactn rate, molecules/ (gr s)	benzene conversn, %	product distribtn, wt %			
			toluene	xylenes	CH <sub>4</sub>	C <sub>2</sub> -C <sub>5</sub>
280	9.2 × 10 <sup>16</sup>	0.4	60		36	4.4
350	1.0 × 10 <sup>18</sup>	1.3	65	3.2	31	1.5
350		16	34	1.0	60	4.8
350		25	26	1.3	68	5.1
380	2.0 × 10 <sup>18</sup>	1.9	64	3.0	32	1.3

<sup>a</sup> At 1 atm, H<sub>2</sub>/Bz = 8 (molar ratio).

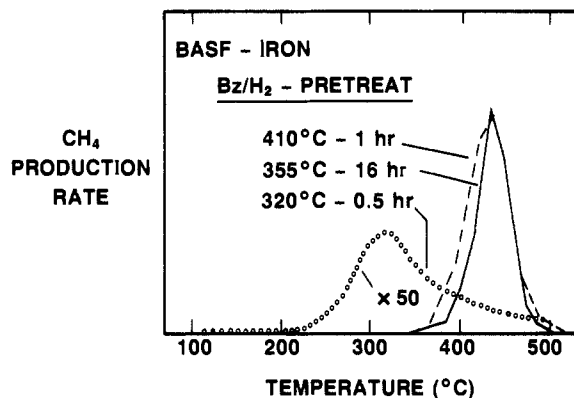


**Figure 1.** TPHT profiles illustrating hydrogenation of carbonaceous species produced during benzene conversion over a fused iron ammonia synthesis catalyst.

ratio for the para:meta:ortho isomers. Consistent with earlier work,<sup>1a,c</sup> hydrogenation to cyclohexane could not be detected. After an initial 1-2-h period of increasing catalytic activity, rates for all reactions gradually declined over many hours.<sup>5</sup>

For benzene conversion levels below 3%, conversion-dependent changes in selectivity were not detected. However, at higher conversions (cf. Table I), selectivity for toluene and xylene production decreased sharply, indicating preferential conversion by secondary hydrogenolysis reactions. Despite this limitation, it is apparent that fused iron displayed unusual selectivity for carbon incorporation.

The hydrogenolysis product distributions suggest a reaction pathway where ring opening is followed by scission of essentially all C-C bonds before rehydrogenation. Reaction of the intermediate CH<sub>x</sub> surface species with an adsorbed benzene derivative produces toluene, whereas complete hydrogenation produces methane. Considering the relative rates of toluene and light alkane production, the probability for carbon reincorporation (rather than hydrogenation to methane) appears to be 0.2-0.3.

The carbon incorporation reaction occurred with extraordinary selectivity for a metal-catalyzed reaction of this type. Previous reports<sup>6</sup> have noted heavier hydrocarbons during alkane hydrogenolysis over Co and Ru, although selectivities for carbon incorporation were only 1-5%. Eckerdt and Bell et al.<sup>7</sup> have also reported reactive scavenging of CH<sub>x</sub> species with cyclohexene and pyridine during Fischer-Tropsch (FT) synthesis over Ru and Fe/SiO<sub>2</sub>. Our studies confirm that CH<sub>x</sub> species are active for reincorporation over a wide range of temperatures exceeding those normally applied in FT synthesis. A common feature of these reactions is their occurrence over FT-active metals implying that similar intermediates participate in both reactions.

Photoemission results showed that iron was well reduced after H<sub>2</sub> activation and remained well reduced after reaction studies. In agreement with earlier work,<sup>8</sup> XPS, LEIS, and CO-chemi-

(1) (a) Yoon, K. J.; Vannice, M. A. *J. Catal.* **1983**, *82*, 457. (b) Yoon, K. J.; Mulay, L. W.; Walker, P. L.; Vannice, M. A. *Ind. Eng. Chem. Prod. Res. Dev.* **1983**, *22*, 519. (c) Norval, G. W.; Phillips, M. J. *J. Catal.* **1989**, *115*, 250. (d) Chou, P.; Vannice, M. A. *J. Catal.* **1987**, *107*, 129. (e) van Meerten, R. Z. C.; Morales, A.; Barbier, J.; Maurel, R. *J. Catal.* **1979**, *58*, 43.

(2) For reviews, see: (a) Davis, S. M.; Somorjai, G. A. In *The Chemical Physics of Solid Surfaces and Heterogeneous Catalysis*; King, D. A., Woodruff, D. P., Eds.; Elsevier: Amsterdam, 1982; Vol. 4, p 217. (b) Peterson, R. J. *Hydrogenation Catalysts*; Noyes Data Corp.: Park Ridge, NJ, 1977; p 129. (c) Anderson, J. R.; Kemball, C. In *Advances in Catalysis*; Eley, D. D., Farkas, A., Eds.; Academic Press: San Diego, 1957; Vol. 9, p 51.

(3) (a) Kubicka, H. *J. Catal.* **1968**, *12*, 223. (b) Freel, J.; Galwey, A. K. *J. Catal.* **1968**, *10*, 277. (c) Phillips, M. J.; Emmett, P. H. *J. Catal.* **1986**, *101*, 268.

(4) (a) Davis, S. M.; Somorjai, G. A. *Bull. Soc. Chim. Fr.* **1985**, 271. (b) Dwyer, D. J. In *Catalyst Characterization Science*; Deviney, M. L., Gland, J. L., Eds.; ACS Symposium Series 288; American Chemical Society: Washington, DC, 1986.

(5) Davis, S. M.; Hudson, C. W., to be published.

(6) (a) Osterloh, W. T.; Cornell, M. E.; Petit, R. *J. Am. Chem. Soc.* **1982**, *104*, 3759. (b) Donahue, C. O.; Clarke, J. K. A.; Rooney, J. *J. Chem. Soc., Faraday Trans. 1* **1980**, *76*, 345.

(7) (a) Eckerdt, J. G.; Bell, A. T. *J. Catal.* **1980**, *62*, 19. (b) Eckerdt, J. G.; Wang, C. J. *J. Catal.* **1983**, *80*, 172. (c) Eckerdt, J. G.; Wang, C. J. *J. Catal.* **1984**, *86*, 239. (d) Anderson, K. G.; Eckerdt, J. G. *J. Catal.* **1985**, *95*, 423.